

Victor A. Kovtunenکو; Ján Eliaš; Pavel Krejčí; Giselle A. Monteiro; Judita Runcziková

Stress-controlled hysteresis and long-time dynamics of implicit differential equations arising in hypoplasticity

Archivum Mathematicum, Vol. 59 (2023), No. 3, 275–286

Persistent URL: <http://dml.cz/dmlcz/151575>

Terms of use:

© Masaryk University, 2023

Institute of Mathematics of the Czech Academy of Sciences provides access to digitized documents strictly for personal use. Each copy of any part of this document must contain these *Terms of use*.



This document has been digitized, optimized for electronic delivery and stamped with digital signature within the project *DML-CZ: The Czech Digital Mathematics Library* <http://dml.cz>

**STRESS-CONTROLLED HYSTERESIS
AND LONG-TIME DYNAMICS OF IMPLICIT DIFFERENTIAL
EQUATIONS ARISING IN HYPOPLASTICITY**

VICTOR A. KOVTUNENKO, JÁN ELIAŠ, PAVEL KREJČÍ, GISELLE A. MONTEIRO,
AND JUDITA RUNCZIKOVÁ

ABSTRACT. A long-time dynamic for granular materials arising in the hypoplastic theory of Kolymbas type is investigated. It is assumed that the granular hardness allows exponential degradation, which leads to the densification of material states. The governing system for a rate-independent strain under stress control is described by implicit differential equations. Its analytical solution for arbitrary inhomogeneous coefficients is constructed in closed form. Under cyclic loading by periodic pressure, finite ratcheting for the void ratio is derived in explicit form, which converges to a limiting periodic process (attractor) when the number of cycles tends to infinity.

1. INTRODUCTION

In this paper we study long-time dynamics of the constitutive stress-strain relation for granular materials like cohesionless soils or broken rocks. The constitutive law is based on the hypoplastic concept proposed by Kolymbas [17], the model is of the rate type and incrementally nonlinear. Compared to hyper- and hypoelastic material laws, the hypoplastic responses are different for loading and unloading, that is typical for inelastic materials. In contrast to the classical elastoplastic concept, the strain is not decomposed into elastic and plastic parts. Physical aspects of hypoplastic models can be found in [26, 27]. For other representatives of incrementally nonlinear constitutive equations, see the models by Armstrong–Frederick [2],

2020 *Mathematics Subject Classification*: primary 34C55; secondary 37N15, 74C15, 74L10.

Key words and phrases: hypoplasticity, rate-independent dynamic system, cyclic behavior, hysteresis, ratcheting, attractor, implicit ODE, closed-form solution, numerical simulation.

Supported by the OeAD Scientific & Technological Cooperation (WTZ CZ18/2020: “Hysteresis in Hypo-Plastic Models”) financed by the Austrian Federal Ministry of Science, Research and Economy (BMWF) and by the Czech Ministry of Education, Youth and Sports (MŠMT), by the GAČR Grant No. 20-14736S, and by the European Regional Development Fund, Project No. CZ.02.1.01/0.0/0.0/16_019/0000778. The Institute of Mathematics of the Czech Academy of Sciences is supported by RVO:67985840. The authors thank Erich Bauer for discussion.

Received August 29, 2022, accepted November 1, 2022. Editor J. Chleboun.

DOI: 10.5817/AM2023-3-275

endochronic [30], octolinear [10], and CLoE [9]. For mathematical modelling granular and multiphase media we cite [1, 11, 12, 13, 22, 23, 24], while for well-posedness analysis we refer to [8, 16, 25].

In an earlier work [7], we have considered the strain-stress law as a nonlinear differential equation for the stress under a given proportional strain (the strain-control). The model therein is a simplified version of the hypoplastic model by Bauer [3] and Gudehus [14], in which the pressure and density dependent properties of granular materials were omitted. In this way we also make a close link to barodesy models [18]. The existence of an exact solution made it possible to describe analytically various scenarios of the behavior of stress paths obtained from monotonic compression, extension, and isochoric deformations [7, 19, 20, 21].

Our ultimate goal in the current work is to study the phenomenon of ratcheting, that is, the shift of the hysteresis loops under periodic loading and unloading cycles. The theoretical ratcheting is infinite when the influence of the void ratio of the granular material is neglected, which is not consistent with experimental observations. In the present paper, we consider a stress-controlled constitutive law within the hypoplastic theory, which allows degradation of the granular hardness. This results in inhomogeneous material parameters, and the granular body becomes asymptotically rigid when the number of cycles tends to infinity. Since we are in the stress-controlled case, the strain rate is the unknown of the problem and has to be found as a solution of an implicit system of differential equations. Like in the strain-controlled case, the solution is found in closed form. Moreover, we prove that the void ratio subjected to periodic loading-unloading pressure cycles converges to an equilibrium, independently of whether the proportional stress paths are isotropic or not.

Within the nonlinear theory of rate-independent materials we consider a constitutive response between the Cauchy stress σ , linearized strain ε , and its rates $\dot{\sigma}$ and $\dot{\varepsilon}$, which is expressed by an implicit function [15, 28]:

$$f(\sigma, \dot{\sigma}, \varepsilon, \dot{\varepsilon}) = 0.$$

For the function f positively homogeneous of degree one with respect to rates:

$$(1.1) \quad f(\sigma, s\dot{\sigma}, \varepsilon, s\dot{\varepsilon}) = sf(\sigma, \dot{\sigma}, \varepsilon, \dot{\varepsilon}) \quad \text{for } s > 0,$$

the constitutive relation is rate-independent. As a special case of f , the hypoplastic law linear with respect to both rates constitutes [29]:

$$(1.2) \quad \dot{\sigma} - \mathbf{L}_4(\sigma)\dot{\varepsilon} = 0,$$

where \mathbf{L}_4 is a fourth-order symmetric tensor. To extend (1.2) for an inelastic behavior such that

$$f(\sigma, \dot{\sigma}, \varepsilon, -\dot{\varepsilon}) \neq -f(\sigma, \dot{\sigma}, \varepsilon, \dot{\varepsilon}),$$

the nonlinearity in $\dot{\varepsilon}$ in the function f can be expressed as

$$(1.3) \quad \dot{\sigma} - \mathbf{L}_4(\sigma)\dot{\varepsilon} - \mathbf{N}(\sigma)\|\dot{\varepsilon}\| = 0,$$

with a second-order symmetric tensor \mathbf{N} and the Frobenius norm $\|\dot{\varepsilon}\| = \sqrt{\dot{\varepsilon} : \dot{\varepsilon}}$.

The hypoplastic law (1.3) satisfying (1.1) arises in engineering by description of granular materials. For cohesionless grains only non-positive principal stresses

$$\sigma_1 \leq 0, \quad \sigma_2 \leq 0, \quad \sigma_3 \leq 0$$

are physically relevant, in that case, the non-negative mechanical pressure reads

$$(1.4) \quad p = -\frac{1}{3}\text{tr}(\boldsymbol{\sigma}) \geq 0, \quad \text{tr}(\boldsymbol{\sigma}) = \sigma_1 + \sigma_2 + \sigma_3 \leq 0.$$

A deformable granular body consists of solid particles of volume V_s assumed constant, and empty voids of variable volume V_v characterized by a void ratio

$$e = \frac{V_v}{V_s} \in (e_d, e_i),$$

whose bounds e_d and e_i depend on the pressure proportionally [4]. More precisely:

$$(1.5) \quad e_d = e_{\min} f_p, \quad e_i = e_{\max} f_p, \quad 0 < e_{\min} < e_{\max}$$

by means of the unified factor

$$(1.6) \quad f_p(p/h_s) = \exp\left(-\left(\frac{3p}{h_s}\right)^n\right) \in (0, \exp(1)], \quad n \geq 0.$$

with $h_s > 0$ denoting the granular hardness. According to [5], h_s allows degradation:

$$\dot{h}_s = \frac{1}{c} (h_s^\infty - h_s), \quad c \geq 0,$$

which is expressed for prescribed $0 < h_s^\infty < h_s^0$ by an exponential function

$$(1.7) \quad h_s(t) = h_s^\infty + (h_s^0 - h_s^\infty) \exp\left(\frac{t_0 - t}{c}\right) \quad \text{for } t > t_0 \geq 0.$$

We assume that the void ratio fulfills the following equation for rates [5]:

$$(1.8) \quad \dot{e} = ne \left(\frac{3p}{h_s}\right)^n \left(\frac{\dot{h}_s}{h_s} - \frac{\dot{p}}{p}\right).$$

For prescribed $p_0 \geq 0$ and $e_0 \in (e_{\min}, e_{\max}) f_p(p_0/h_s^0)$, the solution to (1.8) is expressed in the form akin to (1.5) and (1.6):

$$(1.9) \quad e(p/h_s) = \frac{e_0}{f_p(p_0/h_s^0)} \exp\left(-\left(\frac{3p}{h_s}\right)^n\right) \in (e_d(p/h_s), e_i(p/h_s)).$$

The degradation of granular hardness $h_s(t)$ is shown in the left plot of Figure 1, for the example parameters $h_s^0 = 120$ (MPa), $h_s^\infty = 78.5$ (MPa) and $c = 4$ (h). In the right plot of Figure 1, the void ratio $e_d < e < e_i$ versus p/h_s is drawn, for the example parameters $e_{\min} = 0.1$, $e_0 = 0.2$, $e_{\max} = 0.3$ and $n = 0.82$.

The response relation (1.3) depends on the void ratio e as described next. We will consider the specific model (1.3) due to Bauer [3] and Gudehus [14]:

$$(1.10) \quad \mathbf{L}_4(\boldsymbol{\sigma}) = f_s \left(a^2 \text{tr}(\boldsymbol{\sigma}) \mathbf{I}_4 + \frac{\boldsymbol{\sigma} \otimes \boldsymbol{\sigma}}{\text{tr}(\boldsymbol{\sigma})} \right), \quad \mathbf{N}(\boldsymbol{\sigma}) = f_s f_d a \left(2\boldsymbol{\sigma} - \frac{1}{3} \text{tr}(\boldsymbol{\sigma}) \mathbf{I} \right)$$

using the dyadic product of the stress tensor, where $a > 0$ is the yield strength, while \mathbf{I} and \mathbf{I}_4 stand for the second-order and the forth-order identity tensors,

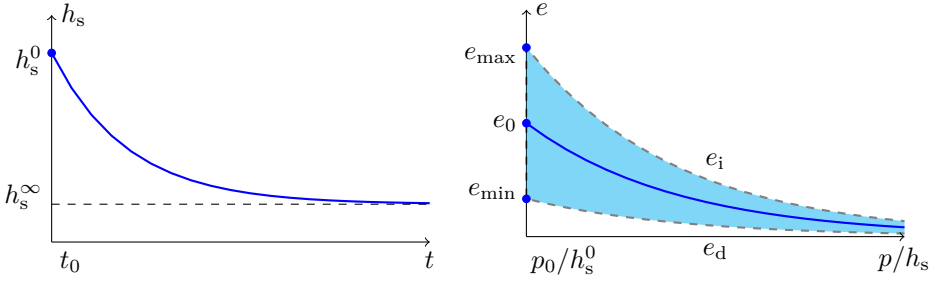


FIG. 1: The granular hardness $h_s(t)$ degradation (left plot); admissible area for void ratio $e_d < e < e_i$ versus p/h_s (right plot).

respectively. The density $f_d > 0$ and stiffness $f_s < 0$ factors depend on the void ratio as follows [4]:

$$(1.11) \quad f_d(e) = \left(\frac{e - e_d}{e_c - e_d} \right)^\alpha, \quad f_s(e) = -b \left(\frac{e_i}{e} \right)^\beta$$

for the parameters $\alpha \in (0, 0.5)$, $\beta > 1$, $b > 0$, and the critical void ratio

$$(1.12) \quad e_c = e_{crt} f_p(p/h_s), \quad e_{\min} < e_{crt} < e_{\max}.$$

Thanks to the identity (1.9) and using the definitions of e_d, e_i in (1.5), one can suppress the void ratio dependence of both functions defined in (1.11), more precisely, the density as well as the stiffness are constants given by

$$(1.13) \quad f_d = \left(\frac{\frac{e_0}{f_p(p_0/h_s^0)} - e_{\min}}{e_{crt} - e_{\min}} \right)^\alpha, \quad f_s = -b \left(\frac{e_{\max} f_p(p_0/h_s^0)}{e_0} \right)^\beta.$$

Inserting (1.10) into (1.3) we write explicitly the differential equation

$$(1.14) \quad \dot{\sigma} = f_s \left\{ a^2 \text{tr}(\sigma) \dot{\varepsilon} + \frac{\dot{\varepsilon} : \sigma}{\text{tr}(\sigma)} \sigma + a f_d \left(2\sigma - \frac{1}{3} \text{tr}(\sigma) \mathbf{I} \right) \|\dot{\varepsilon}\| \right\}.$$

Spatial dependence is omitted from the consideration such that (1.14) implies a coupled system of nonlinear dynamic equations.

2. ANALYSIS OF THE MODEL

In this study we focus on a modeling setup when the strain ε is fully controlled by the stress σ . The stress-controlled proportional loading consists in choosing a fixed second-order symmetric tensor \mathbf{T} such that

$$(2.1) \quad \sigma = s \mathbf{T}, \quad \dot{\sigma} = \dot{s} \mathbf{T},$$

where a loading parameter $s(t) > 0$ is a strictly monotone differentiable function with respect to time $t \in (t_0, t_1)$ for some $0 \leq t_0 < t_1$. This is what we call a *proportional loading* if s is increasing by the mean of $\dot{s} > 0$, and *proportional unloading* if s is decreasing, i.e., $\dot{s} < 0$.

After the substitution of (2.1) into (1.14) we get the implicit system of the first-order ordinary differential equations with respect to the strain rate $\dot{\boldsymbol{\epsilon}}(t)$ as

$$(2.2) \quad \dot{\mathbf{T}} = s f_s \left\{ a^2 \text{tr}(\mathbf{T}) \dot{\boldsymbol{\epsilon}} + \frac{\dot{\boldsymbol{\epsilon}} : \mathbf{T}}{\text{tr}(\mathbf{T})} \mathbf{T} + a f_d \left(2\mathbf{T} - \frac{1}{3} \text{tr}(\mathbf{T}) \mathbf{I} \right) \|\dot{\boldsymbol{\epsilon}}\| \right\},$$

which is under our study. Using for brevity the notation

$$(2.3) \quad \mathbf{X}(t) := \frac{s(t)}{\dot{s}(t)} f_s \dot{\boldsymbol{\epsilon}}, \quad \hat{\mathbf{T}} := \frac{\mathbf{T}}{\text{tr}(\mathbf{T})}, \quad \text{tr}(\hat{\mathbf{T}}) = 1,$$

equation (2.2) after division by $\text{tr}(\mathbf{T})$ turns into

$$(2.4) \quad \hat{\mathbf{T}} = a^2 \mathbf{X} + (\mathbf{X} : \hat{\mathbf{T}}) \hat{\mathbf{T}} \mp a f_d \left(2\hat{\mathbf{T}} - \frac{1}{3} \mathbf{I} \right) \|\mathbf{X}\| \quad \text{for } \pm \dot{s} > 0,$$

with two signs $\mp \|\mathbf{X}\|$ corresponding to $\pm \dot{s} > 0$ due to $f_s < 0$.

Taking the scalar product of (2.4) with \mathbf{X} and gathering like terms we calculate

$$\mathbf{X} : \hat{\mathbf{T}} = \frac{\|\hat{\mathbf{T}}\|^2}{a^2 + \|\hat{\mathbf{T}}\|^2} \pm a f_d \frac{2\|\hat{\mathbf{T}}\|^2 - \frac{1}{3}}{a^2 + \|\hat{\mathbf{T}}\|^2} \|\mathbf{X}\| \quad \text{for } \pm \dot{s} > 0.$$

Its substitution into (2.4) yields

$$\frac{a^2}{a^2 + \|\hat{\mathbf{T}}\|^2} \hat{\mathbf{T}} = a^2 \mathbf{X} \mp a f_d \left(\frac{2a^2 + \frac{1}{3}}{a^2 + \|\hat{\mathbf{T}}\|^2} \hat{\mathbf{T}} - \frac{1}{3} \mathbf{I} \right) \|\mathbf{X}\| \quad \text{for } \pm \dot{s} > 0.$$

Or, after division by a^2 and using for brevity the notation

$$(2.5) \quad \mathbf{A} := \frac{\hat{\mathbf{T}}}{a^2 + \|\hat{\mathbf{T}}\|^2}, \quad \mathbf{B} := \frac{1}{a^2} \left[\left(2a^2 + \frac{1}{3} \right) \mathbf{A} - \frac{1}{3} \mathbf{I} \right],$$

an equivalent equation with respect to \mathbf{X} follows:

$$(2.6) \quad \mathbf{X} = \mathbf{A} \pm a f_d \|\mathbf{X}\| \mathbf{B} \quad \text{for } \pm \dot{s} > 0.$$

Theorem 2.1 (Analytical solution). *Under a solvability condition*

$$(2.7) \quad f_d^2 \leq \frac{1}{a^2 (\|\mathbf{B}\|^2 - (\frac{\mathbf{A} : \mathbf{B}}{\|\mathbf{A}\|})^2)} = \frac{3a^2 \|\hat{\mathbf{T}}\|^2}{\|\hat{\mathbf{T}}\|^2 - \frac{1}{3}} =: f_{\max},$$

a solution to the nonlinear system (2.6) is given in the closed form:

$$(2.8) \quad \mathbf{X} = \mathbf{A} + \frac{a f_d \|\mathbf{A}\| \mathbf{B}}{\pm \sqrt{D} - a f_d \frac{\mathbf{A} : \mathbf{B}}{\|\mathbf{A}\|}} \quad \text{for } \pm \dot{s} > 0,$$

or, explicitly in terms of $\hat{\mathbf{T}}$:

$$(2.9) \quad \mathbf{X} = \frac{\pm \|\hat{\mathbf{T}}\| \sqrt{D} \hat{\mathbf{T}} - \frac{1}{3a} f_d (\|\hat{\mathbf{T}}\|^2 \mathbf{I} - \hat{\mathbf{T}})}{\pm \|\hat{\mathbf{T}}\| (a^2 + \|\hat{\mathbf{T}}\|^2) \sqrt{D} - a f_d (2\|\hat{\mathbf{T}}\|^2 - \frac{1}{3})}, \quad D := 1 - \frac{f_d^2}{f_{\max}}.$$

Proof. Taking the norm of the expression (2.6) we get

$$\|\mathbf{X}\|^2 = \|\mathbf{A} \pm a f_d \|\mathbf{X}\| \mathbf{B}\|^2 = \|\mathbf{A}\|^2 \pm 2a f_d (\mathbf{A} : \mathbf{B}) \|\mathbf{X}\| + a^2 f_d^2 \|\mathbf{B}\|^2 \|\mathbf{X}\|^2,$$

which turns into the quadratic equation with respect to $\lambda = \|\mathbf{X}\|$:

$$(2.10) \quad (1 - a^2 f_d^2 \|\mathbf{B}\|^2) \lambda^2 \mp 2a f_d (\mathbf{A} : \mathbf{B}) \lambda - \|\mathbf{A}\|^2 = 0 \quad \text{for } \pm \dot{s} > 0,$$

where according to (2.5)

$$(2.11) \quad \|\mathbf{A}\| = \frac{\|\hat{\mathbf{T}}\|}{a^2 + \|\hat{\mathbf{T}}\|^2}, \quad \text{tr}(\mathbf{A}) = \frac{1}{a^2 + \|\hat{\mathbf{T}}\|^2},$$

and the coefficients are

$$(2.12) \quad \mathbf{A} : \mathbf{B} = \left(2 + \frac{1}{3a^2}\right)\|\mathbf{A}\|^2 - \frac{\text{tr}(\mathbf{A})}{3a^2} = \frac{2\|\hat{\mathbf{T}}\|^2 - \frac{1}{3}}{(a^2 + \|\hat{\mathbf{T}}\|^2)^2},$$

$$\|\mathbf{B}\|^2 = \left(2 + \frac{1}{3a^2}\right)\left(\mathbf{A} : \mathbf{B} - \frac{\text{tr}(\mathbf{A})}{3a^2}\right) + \frac{1}{3a^4} = \left(2 + \frac{1}{3a^2}\right)\frac{(2 - \frac{1}{3a^2})\|\hat{\mathbf{T}}\|^2 - \frac{2}{3}}{(a^2 + \|\hat{\mathbf{T}}\|^2)^2} + \frac{1}{3a^4}.$$

The discriminant for this equation

$$(2.13) \quad \text{Disc} = \|\mathbf{A}\|^2 \left(1 - a^2 f_d^2 \left[\|\mathbf{B}\|^2 - \left(\frac{\mathbf{A} : \mathbf{B}}{\|\mathbf{A}\|}\right)^2\right]\right) = \frac{\|\hat{\mathbf{T}}\|^2 - \frac{1}{3a^2} f_d^2 (\|\hat{\mathbf{T}}\|^2 - \frac{1}{3})}{(a^2 + \|\hat{\mathbf{T}}\|^2)^2}$$

is non-negative when the solvability condition (2.7) holds, provided by the lower bound $\|\hat{\mathbf{T}}\|^2 \geq 1/3$ since $\text{tr}(\hat{\mathbf{T}}) = 1$. Then the roots of (2.10) are

$$(2.14) \quad \lambda = \frac{\pm a f_d (\mathbf{A} : \mathbf{B}) + \sqrt{\text{Disc}}}{1 - a^2 f_d^2 \|\mathbf{B}\|^2}, \quad \lambda = \frac{\pm a f_d (\mathbf{A} : \mathbf{B}) - \sqrt{\text{Disc}}}{1 - a^2 f_d^2 \|\mathbf{B}\|^2}$$

for $\pm \dot{s} > 0$. Since $\|\mathbf{X}\|$ has a sense only for positive values of λ , noting that $\mathbf{A} : \mathbf{B} > 0$ in (2.12) and using (2.13) to write

$$1 - a^2 f_d^2 \|\mathbf{B}\|^2 = \frac{(\sqrt{\text{Disc}})^2 - (a f_d (\mathbf{A} : \mathbf{B}))^2}{\|\mathbf{A}\|^2},$$

from (2.14) we deduce

$$(2.15) \quad \|\mathbf{X}\| = \frac{\|\mathbf{A}\|^2}{\sqrt{\text{Disc}} \mp a f_d (\mathbf{A} : \mathbf{B})} > 0 \quad \text{for } \pm \dot{s} > 0.$$

The substitution of (2.15) into (2.6) gives the analytical formulas (2.8) and (2.9) for the solution, where $D = \text{Disc}/\|\mathbf{A}\|^2$ from (2.13). This finishes the proof. \square

Note that the expressions obtained in Theorem 2.1 show no dependence in time resulting in a constant value for X implicitly related to the loading parameter. The formulas above together with (2.3) allow us to derive the strain rate in terms of \mathbf{X} provided $f_d^2 \leq f_{\max}$, in other words, equation (2.3) gives

$$(2.16) \quad \dot{\epsilon} = \frac{\dot{s}}{s f_s} \mathbf{X},$$

and from (2.9) we infer the scalar expression

$$(2.17) \quad \text{tr}(\dot{\epsilon}) = \left(\frac{\dot{s}}{s f_s}\right) \frac{\pm \|\hat{\mathbf{T}}\| \sqrt{1 - \frac{f_d^2}{f_{\max}^2}} - \frac{1}{a} f_d (\|\hat{\mathbf{T}}\|^2 - \frac{1}{3})}{\pm \|\hat{\mathbf{T}}\| (a^2 + \|\hat{\mathbf{T}}\|^2) \sqrt{1 - \frac{f_d^2}{f_{\max}^2}} - a f_d (2\|\hat{\mathbf{T}}\|^2 - \frac{1}{3})}$$

for $\pm \dot{s} > 0$, which we use for numerical simulation tests below.

2.1. **Isotropic loading.** In particular, for the isotropic case

$$(2.18) \quad \mathbf{T} = -\mathbf{I}, \quad \text{tr}(\mathbf{T}) = -3, \quad \hat{\mathbf{T}} = \frac{1}{3}\mathbf{I}, \quad \|\hat{\mathbf{T}}\| = \frac{1}{\sqrt{3}},$$

then $f_{\max} = \infty$ and $D = 1$, thus (2.7) always holds. From (2.9) we have

$$(2.19) \quad \mathbf{X} = \frac{1}{3a^2 + 1 \mp \sqrt{3}af_d} \mathbf{I} \quad \text{for } \pm \dot{s} > 0,$$

and from (2.17) get respectively

$$(2.20) \quad \text{tr}(\mathbf{X}) = \frac{3}{3a^2 + 1 \mp \sqrt{3}af_d} \quad \text{for } \pm \dot{s} > 0.$$

2.2. **Example of shear stress.** Let us consider the shear stress matrix

$$(2.21) \quad \mathbf{T} = \begin{bmatrix} -0.5 & 0.5 & 0 \\ 0.5 & -0.5 & 0 \\ 0 & 0 & 0 \end{bmatrix}, \quad \text{tr}(\mathbf{T}) = -1, \quad \hat{\mathbf{T}} = -\mathbf{T}, \quad \|\hat{\mathbf{T}}\| = 1$$

such that the principal stresses $\sigma_1 = -1$, $\sigma_2 = \sigma_3 = 0$, and $f_{\max} = 4.5a^2$ in (2.7). Let us consider the functions in (1.11) rescaled as follows

$$(2.22) \quad f_d(e/f_p) = \left(\frac{e/f_p - e_{\min}}{e_{\text{crt}} - e_{\min}} \right)^\alpha, \quad f_s(e/f_p) = -b \left(\frac{e_{\max}}{e/f_p} \right)^\beta.$$

From (2.17) and (2.22) we find

$$(2.23) \quad \frac{1}{f_s} \text{tr}(\mathbf{X}) = \frac{1}{f_s} \frac{\pm \sqrt{1 - \frac{2f_d^2}{9a^2}} - \frac{2}{3a} f_d}{\pm (a^2 + 1) \sqrt{1 - \frac{2f_d^2}{9a^2}} - \frac{5a}{3} f_d} \quad \text{for } \pm \dot{s} > 0$$

as a function of two variables a and $e/f_p \in [e_{\min}, e_{\max}]$.

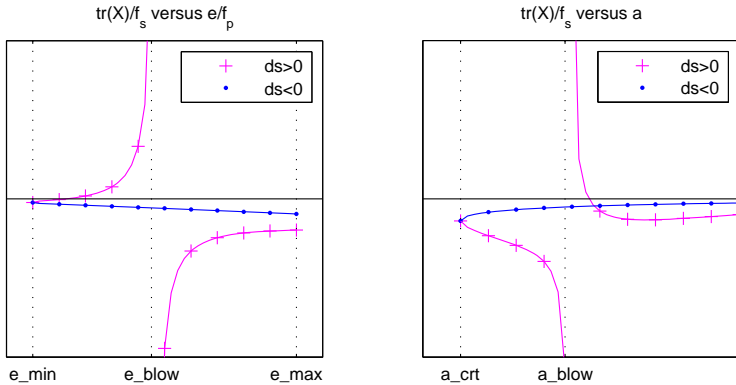


FIG. 2: Example $\text{tr}(\mathbf{X})/f_s$ for $\pm \dot{s} > 0$ versus parameter e/f_p entering f_d and f_s (left plot); versus yield strength a (right plot).

For the parameters used in Figure 1 and $\alpha = 0.18$, $\beta = 1.05$, $b = 1$, two graphs of $\text{tr}(\mathbf{X})/f_s$ for $\dot{s} > 0$ and $\dot{s} < 0$ versus e/f_p and fixed $a = 0.6$ are depicted in the window $|\text{tr}(\mathbf{X})/f_s| \leq 10$ in the left plot of Figure 2. They coincide at $e/f_p = e_{\min}$ because $f_d = 0$ and $\mathbf{X} = \mathbf{A}$ in (2.8) is unique in this case. The graph as $\dot{s} < 0$ is continuous, whereas as $\dot{s} > 0$ it blows up when the denominator in (2.23), that is,

$$(2.24) \quad \|\hat{\mathbf{T}}\|(a^2 + \|\hat{\mathbf{T}}\|^2) \sqrt{1 - \frac{f_d^2}{f_{\max}}} - a f_d \left(2\|\hat{\mathbf{T}}\|^2 - \frac{1}{3}\right),$$

tends to zero at $e_{\text{blow}} \approx 0.19$.

In the right plot of Figure 2, two graphs of $\text{tr}(\mathbf{X})/f_s$ for $\pm \dot{s} > 0$ are depicted versus the yield strength $a \geq a_{\text{crt}}$ in the window $|\text{tr}(\mathbf{X})/f_s| \leq 10$ and $a \leq 1.2$ for fixed $e/f_p = e_0/f_p(p_0/h_s^0) \approx 0.2278$ used in Figure 1. There $a_{\text{crt}} \approx 0.4638$ can be found from the solvability condition (2.7) such that

$$(2.25) \quad a_{\text{crt}} = \frac{\sqrt{\|\hat{\mathbf{T}}\|^2 - \frac{1}{3}}}{\sqrt{3}\|\hat{\mathbf{T}}\|} f_d.$$

When (2.25) holds, the corresponding discriminant $D = 0$ and the solution $\mathbf{X} = \mathbf{A} + \|\mathbf{A}\|^2 \mathbf{B}/(\mathbf{A} : \mathbf{B})$ in (2.8) is unique for both $\pm \dot{s} > 0$. As $\dot{s} > 0$ the denominator in (2.24) tends to zero and causes the blow up at $a_{\text{blow}} \approx 0.7398$.

3. HYSTERESIS UNDER CYCLIC LOADING

Let us consider a time discretization based on equidistant points $t_k = k\tau$ for $k = 0, 1, 2, \dots$ and a fixed period $\tau > 0$. For prescribed $0 < s_{\text{even}} \leq s(t_0) < s_{\text{odd}}$, we introduce cyclic loading by a continuous periodic function $s(t)$ in (2.1) such that

$$(3.1) \quad \begin{cases} \dot{s} > 0 & \text{for } t \in (t_{2j}, t_{2j+1}), \\ \dot{s} < 0 & \text{for } t \in (t_{2j+1}, t_{2j+2}), \end{cases} \quad j = 0, 1, 2, \dots$$

where the node values for the loading parameter are set

$$(3.2) \quad s(t_2) = s(t_4) = \dots = s_{\text{even}}, \quad s(t_1) = s(t_3) = \dots = s_{\text{odd}}.$$

For example, solving the equation $\dot{s} = s$ with $s(t_0) = s_{\text{even}}$ we get

$$(3.3) \quad \begin{cases} s(t) = s(t_{2j}) \exp(t - t_{2j}) & \text{for } t \in (t_{2j}, t_{2j+1}), \\ s(t) = s(t_{2j+1}) \exp(t_{2j+1} - t) & \text{for } t \in (t_{2j+1}, t_{2j+2}), \end{cases}$$

which is continuous when $s_{\text{odd}} = s_{\text{even}} \exp(\tau)$ and is illustrated in Figure 3. Having in mind the identities in (2.1) with the cyclic loading described by (3.1) and (3.2), the corresponding equation for the mechanical pressure (1.4) becomes

$$(3.4) \quad p(t) = -s(t) \frac{\text{tr}(\mathbf{T})}{3} \quad \text{for } t \in (t_{2j}, t_{2j+1}) \cup (t_{2j+1}, t_{2j+2}),$$

therefore, it is continuous and periodic with

$$(3.5) \quad p(t_{2j+2}) = -s_{\text{even}} \frac{\text{tr}(\mathbf{T})}{3} =: p_{\text{even}}, \quad p(t_{2j+1}) = -s_{\text{odd}} \frac{\text{tr}(\mathbf{T})}{3} =: p_{\text{odd}},$$

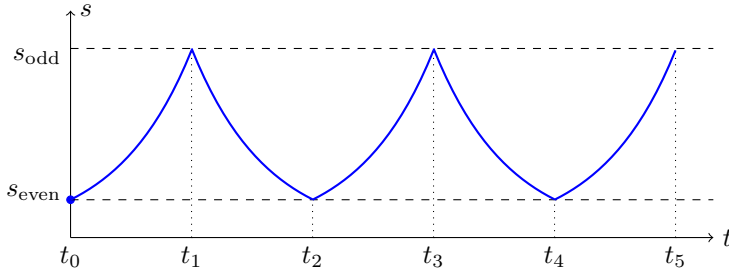


FIG. 3: Example cyclic loading $s(t)$.

where $0 < p_{\text{even}} \leq p(t_0) < p_{\text{odd}}$ because of $\text{tr}(\mathbf{T}) \leq 0$ in (1.4). The granular hardness in (1.7) after discretization implies a monotonically decaying sequence

$$(3.6) \quad h_s(t_k) = h_s^\infty + (h_s^0 - h_s^\infty) \exp\left(\frac{t_0 - t_k}{c}\right) \searrow h_s^\infty \quad \text{as } k \rightarrow \infty.$$

For the pressure and granular hardness-dependent function $f_p(p/h_s)$ defined in (1.6), let the initial void ratio be prescribed at $t = t_0$:

$$e(t_0) \in (e_{\min}, e_{\max}) f_p(p(t_0)/h_s(t_0)).$$

The void ratio in (1.9) yields a time-dependent relation as $k = 0, 1, 2, \dots$

$$(3.7) \quad e(t) = \frac{e(t_k)}{f_p(p(t_k)/h_s(t_k))} f_p(p(t)/h_s(t)) \quad \text{for } t \in (t_k, t_{k+1}).$$

The function in (3.7) is continuous at $t = t_{k+1}$. The factors in (1.13) are determined by $e_0 = e(t_0)$, $p_0 = p(t_0)$, and $h_s^0 = h_s(t_0)$.

Assuming that $f_d^2 \leq f_{\max}$ according to (2.7) in Theorem 2.1, from (2.8) and (2.16) we get the strain rate for $j = 0, 1, 2, \dots$

$$(3.8) \quad \begin{cases} \dot{\epsilon}(t) = \frac{\dot{s}(t)}{s(t)f_s} \left(\mathbf{A} + \frac{af_d \|\mathbf{A}\| \mathbf{B}}{\sqrt{1 - \frac{f_d^2}{f_{\max}} - af_d \frac{\mathbf{A}:\mathbf{B}}{\|\mathbf{A}\|}}} \right) & \text{for } t \in (t_{2j}, t_{2j+1}), \\ \dot{\epsilon}(t) = \frac{\dot{s}(t)}{s(t)f_s} \left(-\mathbf{A} + \frac{af_d \|\mathbf{A}\| \mathbf{B}}{\sqrt{1 - \frac{f_d^2}{f_{\max}} + af_d \frac{\mathbf{A}:\mathbf{B}}{\|\mathbf{A}\|}}} \right) & \text{for } t \in (t_{2j+1}, t_{2j+2}). \end{cases}$$

Theorem 3.1 (Attractor). *Under the stress control (2.1) by cyclic loading (3.1) and (3.2) the void ratio is found in the closed form:*

$$(3.9) \quad e(t) = e(t_0) \exp\left((-\text{tr}(\mathbf{T}))^n \left[\left(\frac{s(t_0)}{h_s(t_0)} \right)^n - \left(\frac{s(t)}{h_s(t)} \right)^n \right] \right) \quad \text{for } t \geq t_0.$$

As $t \rightarrow \infty$ it tends exponentially to an attractor with end-points

$$(3.10) \quad e_i^\infty = e(t_0) \exp\left((-\text{tr}(\mathbf{T}))^n \left[\left(\frac{s(t_0)}{h_s(t_0)} \right)^n - \left(\frac{s_i}{h_s^\infty} \right)^n \right] \right) \quad \text{for } i \in \{\text{even}, \text{odd}\}.$$

Proof. From (3.7), the following formula can be justified by induction:

$$(3.11) \quad e(t_k) = \frac{e(t_0)}{f_p(p(t_0)/h_s(t_0))} f_p(p(t_k)/h_s(t_k)) \quad \text{for } k = 0, 1, 2, \dots$$

Inserting here (1.6), (3.5) and (3.6) we calculate the void ratio (3.9). Based on the periodicity (3.2) and convergence (3.6), the assertion follows. \square

3.1. Example of densification. Under the cyclic loading given by (3.3) for $s_{\text{even}} = 1$, $\tau = 1$, and $s(t_0) = s_{\text{odd}} = \exp(1) \approx 2.7183$, we put $\text{tr}(\mathbf{T}) = -1$ from the example stress (2.21) such that the pressure bounds $p_{\text{even}} \approx 0.3333$ and $p(t_0) = p_{\text{odd}} \approx 0.9061$ in (3.5). The graph of the void ratio $e(t)$ computed by formula (3.9) is drawn versus $p(t)$ in Figure 4 after 10 cycles implying $j = 0, 1, \dots, 9$ in (3.1) with t_0, t_1, \dots, t_{19} time points. The consequential cycles of $e(t)$ are visually indistinguishable and approach the attractor according to Theorem 3.1.

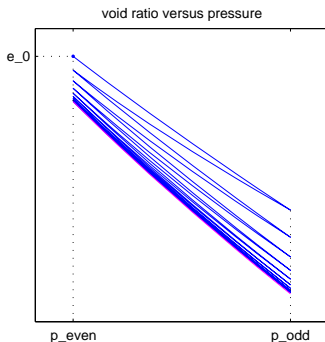


FIG. 4: Void ratio $e(t)$ versus pressure $p(t)$ under cyclic loading.

4. CONCLUSION

We conclude with some principal findings of our theoretical and numerical study.

- An implicit system of 1st-order ordinary differential equations is studied to model a granular media within the hypoplastic theory, which allows degradation of
- Under stress control, an analytical formula for the strain rate is constructed for arbitrary inhomogeneous coefficients in the governing equations.
- Under loading-unloading cycles, the void ratio exhibits ratcheting of hysteresis loops towards densification of the granular media.
- The ratcheting phenomenon is finite, pressure-void ratio states generate an attractor with respect to time.

REFERENCES

- [1] Annin, B.D., Kovtunenکو, V.A., Sadovskii, V.M., *Variational and hemivariational inequalities in mechanics of elastoplastic, granular media, and quasibrittle cracks*, Analysis, Modelling, Optimization, and Numerical Techniques (Tost, G.O., Vasilieva, O., eds.), vol. 121, Springer Proc. Math. Stat., 2015, pp. 49–56.
- [2] Armstrong, P.J., Frederick, C.O., *A mathematical representation of the multiaxial Bauschinger effect*, C.E.G.B. Report RD/B/N, 1966.
- [3] Bauer, E., *Calibration of a comprehensive hypoplastic model for granular materials*, Soils Found. **36** (1996), 13–26.
- [4] Bauer, E., *Analysis of shear band bifurcation with a hypoplastic model for a pressure and density sensitive granular material*, Mech. Mater. **31** (1999), 597–609.
- [5] Bauer, E., *Long-term behavior of coarse-grained rockfill material and their constitutive modeling*, Dam Engineering - Recent Advances in Design and Analysis (Fu, Z., Bauer, E., eds.), IntechOpen, 2021.
- [6] Bauer, E., Kovtunenکو, V.A., Krejčí, P., Krenn, N., Siváková, L., Zubkova, A.V., *Modified model for proportional loading and unloading of hypoplastic materials*, Extended Abstracts Spring 2018. Singularly Perturbed Systems, Multiscale Phenomena and Hysteresis: Theory and Applications (Korobeinikov, A., Caubergh, M., Lázaro, T., Sardanyés, J., eds.), Trends in Mathematics, vol. 11, Birkhäuser, Hamburg, 2019, pp. 201–210.
- [7] Bauer, E., Kovtunenکو, V.A., Krejčí, P., Krenn, N., Siváková, L., Zubkova, A.V., *On proportional deformation paths in hypoplasticity*, Acta Mechanica **231** (2020), 1603–1619.
- [8] Brokate, M., Krejčí, P., *Wellposedness of kinematic hardening models in elastoplasticity*, RAIRO Modél. Math. Anal. Numér. **32** (1998), 177–209.
- [9] Chambon, R., Desrues, J., Hammad, W., Charlier, R., *CLoE, a new rate-type constitutive model for geomaterials, theoretical basis and implementation*, Int. J. Num. Anal. Methods Geomech. **18** (1994), 253–278.
- [10] Darve, F., *Incrementally non-linear constitutive relationships*, Geomaterials, Constitutive Equations and Modelling (Darve, F., ed.), Elsevier, Horton, Greece, 1990, pp. 213–238.
- [11] Fellner, K., Kovtunenکو, V.A., *A singularly perturbed nonlinear Poisson–Boltzmann equation: uniform and super-asymptotic expansions*, Math. Methods Appl. Sci. **38** (2015), 3575–3586.
- [12] Fellner, K., Kovtunenکو, V.A., *A discontinuous Poisson–Boltzmann equation with interfacial transfer: homogenisation and residual error estimate*, Appl. Anal. **95** (2016), 2661–2682.
- [13] González Granada, J.R., Kovtunenکو, V.A., *Entropy method for generalized Poisson–Nernst–Planck equations*, Anal. Math. Phys. **8** (2018), 603–619.
- [14] Gudehus, G., *A comprehensive constitutive equation for granular materials*, Soils Found. **36** (1996), 1–12.
- [15] Hron, J., Málek, J., Rajagopal, K.R., *Simple flows of fluids with pressure dependent viscosities*, Proc. Roy. Soc. A **457** (2001), 1603–1622.
- [16] Khudnev, A.M., Kovtunenکو, V.A., *Analysis of Cracks in Solids*, WIT-Press, Southampton, Boston, 2000.
- [17] Kolymbas, D., *Introduction to Hypoplasticity*, A.A. Balkema, Rotterdam, 2000.
- [18] Kolymbas, D., Medicus, G., *Genealogy of hypoplasticity and barodesy*, Int. J. Numer. Anal. Methods Geomech. **40** (2016), 2530–2550.
- [19] Kovtunenکو, V.A., Bauer, E., Eliaš, J., Krejčí, P., Monteiro, G.A., Straková (Siváková), L., *Cyclic behavior of simple models in hypoplasticity and plasticity with nonlinear kinematic hardening*, J. Sib. Fed. Univ. - Math. Phys. **14** (2021), 756–767.
- [20] Kovtunenکو, V.A., Krejčí, P., Bauer, E., Siváková, L., Zubkova, A.V., *On Lyapunov stability in hypoplasticity*, Proc. Equadiff 2017 Conference (Mikula, K., Ševčovič, D., Urbán, J., eds.), Slovak University of Technology, Bratislava, 2017, pp. 107–116.

- [21] Kovtunenکو, V.A., Krejčí, P., Krenn, N., Bauer, E., Siváková, L., Zubkova, A.V., *On feasibility of rate-independent stress paths under proportional deformations within hypoplastic constitutive model for granular materials*, Math. Models Eng. **5** (2019), 119–126.
- [22] Kovtunenکو, V.A., Zubkova, A.V., *Mathematical modeling of a discontinuous solution of the generalized Poisson–Nernst–Planck problem in a two-phase medium*, Kinet. Relat. Models **11** (2018), 119–135.
- [23] Kovtunenکو, V.A., Zubkova, A.V., *Homogenization of the generalized Poisson–Nernst–Planck problem in a two-phase medium: correctors and estimates*, Appl. Anal. **100** (2021 a), 253–274.
- [24] Kovtunenکو, V.A., Zubkova, A.V., *Existence and two-scale convergence of the generalised Poisson–Nernst–Planck problem with non-linear interface conditions*, Eur. J. Appl. Math. **32** (2021 b), 683–710.
- [25] Krejčí, P., *Hysteresis, Convexity and Dissipation in Hyperbolic Equations*, Gakkotosho, Tokyo, 1996.
- [26] Mašín, D., *Modelling of Soil Behaviour with Hypoplasticity: Another Approach to Soil Constitutive Modelling*, Springer Nature, Switzerland, 2019.
- [27] Niemunis, A., Herle, I., *Hypoplastic model for cohesionless soils with elastic strain range*, Mech. Cohes.-Fric. Mat. **2** (1997), 279–299.
- [28] Rajagopal, K.R., Srinivasa, A.R., *On a class of non-dissipative materials that are not hyperelastic*, Proc. Roy. Soc. A **465** (2009), 493–500.
- [29] Truesdell, C., *Remarks on hypo-elasticity*, J. Res. Natl. Bur. Stand. B **67B** (1963), 141–143.
- [30] Valanis, K.C., *A theory of viscoplasticity without a yield surface*, Arch. Mech. **23** (1971), 517–533.

INSTITUTE FOR MATHEMATICS AND SCIENTIFIC COMPUTING,
UNIVERSITY OF GRAZ, NAWI GRAZ,
HEINRICHSTR. 36, 8010 GRAZ, AUSTRIA
AND

LAVRENT'EV INSTITUTE OF HYDRODYNAMICS,
SIBERIAN DIVISION OF THE RUSSIAN ACADEMY OF SCIENCES,
630090 NOVOSIBIRSK, RUSSIA
E-mail: victor.kovtunenکو@uni-graz.at

INSTITUTE FOR MATHEMATICS AND SCIENTIFIC COMPUTING,
UNIVERSITY OF GRAZ, NAWI GRAZ,
HEINRICHSTR. 36, 8010 GRAZ, AUSTRIA
E-mail: jan.elias3@gmail.com

FACULTY OF CIVIL ENGINEERING,
CZECH TECHNICAL UNIVERSITY IN PRAGUE,
THÁKUROVA 7, 166 29 PRAHA 6, CZECH REPUBLIC
E-mail: krejci@math.cas.cz

INSTITUTE OF MATHEMATICS, CZECH ACADEMY OF SCIENCES,
ŽITNÁ 25, 115 67 PRAHA 1, CZECH REPUBLIC
E-mail: gam@math.cas.cz

FACULTY OF CIVIL ENGINEERING,
CZECH TECHNICAL UNIVERSITY IN PRAGUE,
THÁKUROVA 7, 166 29 PRAHA 6, CZECH REPUBLIC
E-mail: judita.runczikova@fsv.cvut.cz